Perpendicular magnetic tunnel junction with W seed and capping layers

H. Almasi,[1] C. L. Sun,[2] X. Li,[3] T. Newhouse-Illige,[1] C. Bi,[1] K. C. Price,[1] S. Nahar,[4] C. Grezes,[3] Q. Hu,[5] P. Khalili Amiri,[3,5] K. L. Wang,[3] P. M. Voyles,[2] and W. G. Wang[1,a)]
[1]*Department of Physics, University of Arizona, Tucson, Arizona 85721, USA*
[2]*Department of Materials Science and Engineering, University of Wisconsin, Madison 53706, USA*
[3]*Department of Electrical Engineering, University of California, Los Angeles, California 90095, USA*
[4]*Science Department, Sunnyside High School, Tucson, Arizona 85706, USA*
[5]*Inston, Inc., Los Angeles, California 90024, USA*

(Received 8 February 2017; accepted 7 April 2017; published online 20 April 2017)

We present a study on perpendicular magnetic tunnel junctions with W as buffer and capping layers. A tunneling magnetoresistance of 138% and an interfacial magnetic anisotropy of 1.67 erg/cm^2 were obtained in optimally annealed samples. However, after extended annealing at 420 °C, junctions with W layers showed extremely small resistance due to interdiffusion of W into the MgO barrier. In contrast, in Ta-based junctions, the MgO barrier remained structurally stable despite disappearance of magnetoresistance after extended annealing due to loss of perpendicular magnetic anisotropy. Compared with conventional tunnel junctions with in-plane magnetic anisotropy, the evolution of tunneling conductance suggests that the relatively low magnetoresistance in perpendicular tunnel junctions is related to the lack of highly polarized Δ_1 conducting channel developed in the initial stage of annealing. *Published by AIP Publishing*. [http://dx.doi.org/10.1063/1.4981878]

INTRODUCTION

Perpendicular magnetic tunnel junction (pMTJ) is one of the best candidates for next generation spintronic memory and logic applications. Usually the perpendicular easy axis in pMTJs is provided by materials with bulk perpendicular magnetic anisotropy (PMA) with rare-earth or L1$_0$ magnetic alloys,[1,2] by exchange coupled ferromagnetic electrode with a Co/Pt (Pd) superlattice,[3,4] or by interfacial PMA in heavy-metal/ferromagnet/oxide (HM/FM/oxide) structures.[5–7] In addition to support a reasonably large PMA and tunneling magnetoresistance (TMR), the simple HM/FM/oxide structure may also enable ultra-low energy switching of pMTJ[8–10] through effects such as voltage controlled magnetic anisotropy (VCMA)[11–14] and voltage controlled magnetism.[15,16] In most HM/FM/oxide structures, CoFeB (CFB) and MgO are the preferred materials in order to obtain large TMR.[17,18] For many practical applications pMTJs need to maintain their structure integrity at 400 °C or above.[19,20] Therefore the very thin thickness of CoFeB (~1 nm) puts stringent requirements on the choice of HM layer. Ta has been widely used due to its high thermal stability, ability to absorb Boron, and nearly amorphous crystalline structure.[6,13,18] Other HMs such as Pt (Pd),[21] Hf,[22–24] and Mo[7,25–27] have also been explored in pMTJs. A few experiments have shown that large PMA can be obtained in W/CoFeB/MgO,[28–31] suggesting W could be a good candidate for pMTJs. A TMR of 60% was achieved in hybrid junctions with a perpendicular W/CoFeB bottom electrode and an in-plane top electrode,[32] and pMTJs with (Co/Pt)$_n$/W/CoFeB electrodes have been recently reported.[33,34] However, TMR in fully perpendicular junctions with simple W/CoFeB/MgO structure has not been reported.

In this work, we report a TMR of 138% in full pMTJs with W as the buffer and capping layers. We investigated the evolution of tunneling conductance and TMR during the annealing process in pMTJ with W and Ta layers. It was found that although pMTJs with W layers could maintain better PMA during prolonged annealing, the diffusion of W into the CoFeB/MgO/CoFeB layer has progressively deteriorated the tunneling barrier, leading to the collapse of junction resistance. Furthermore, through the comparison with conventional tunnel junctions with in-plane magnetic anisotropy, the evolution of tunneling conductance suggests the relatively low TMR in pMTJs is related to the lack of highly polarized Δ_1 conducting channel developed in the initial stage of annealing.

EXPERIMENT

All samples in this work were deposited on silicon wafers with 300 nm of thermal oxide in a 12-source magnetron sputtering system (AJA-International). The base pressure is in the range of 10^{-9} Torr, and the working pressure is about 2 mT of Ar for the metallic layers and 1.1 mTorr for MgO layer. Metallic layers and MgO layer were deposited by DC and RF magnetron sputtering, respectively. The substrates were held at room temperature during deposition. For transport studies, multilayers consisting of W(6)/Ru(10)/W(9)/$Co_{20}Fe_{60}B_{20}$(0.8–0.95)/MgO(1.5–3)/$Co_{20}Fe_{60}B_{20}$(1.5–1.6)/W(9)/Ru(20) and Ta(6)/Ru(10)/Ta(9)/$Co_{20}Fe_{60}B_{20}$(0.85)/MgO(1.5–3)/$Co_{20}Fe_{60}B_{20}$(1.6)/Ta(9)/Ru(20) were used, where the numbers in parentheses indicate the thickness in nanometers. The samples were annealed in a rapid thermal annealing setup for various annealing temperatures. Multilayer films were patterned into circular MTJs with diameters of 3–20 μm using conventional microfabrication techniques for TMR measurements. The magnetic properties of unpatterned films were characterized

a)wgwang@physics.arizona.edu

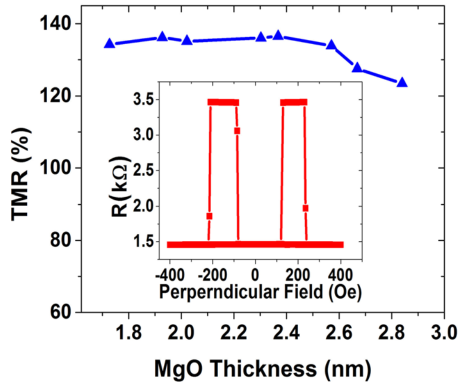

FIG. 1. TMR ratio in W-pMTJs with different MgO thickness annealed for 10 min at 420 °C. The structure of this series of samples is Si/SiO_2/W(6)/Ru(10)/W(9)/CoFeB(0.95)/MgO(1.8-3)/CoFeB(1.5)/W(9)/Ru(20). The inset shows the highest TMR of 138% achieved in this study.

by a vibrating sample magnetometer (VSM) and independently verified by a superconducting quantum interference device (SQUID). The microstructure of pMTJs with W and Ta layers was investigated by sub-angstrom resolution scanning transmission electron microscopy (STEM) performed in FEI Titan STEM with CEOS probe aberration corrector.

RESULTS AND DISCUSSION

It is known that an essential step to obtain high TMR in CoFeB/MgO/CoFeB sandwiches is a post-deposition thermal treatment by annealing junctions at a high temperature.[18,35] In conventional pMTJs with Ta/CoFeB/MgO structures, annealing at high temperatures above 300 °C could lead to the loss of well-defined antiparallel state and therefore a dramatic drop of TMR.[36,37] Hence, an appropriate annealing condition (i.e., annealing time and temperature) is critical to optimize TMR and PMA in perpendicular tunnel junctions. For our W-pMTJs, it was found that annealing at 420 °C for 10 min gave rise to the highest TMR values with a strong PMA. The TMR of a series of pMTJs with different MgO barrier thickness annealed under this condition is plotted in Fig. 1. Large magnetoresistance ratio above 125% was observed for the entire range. The highest TMR obtained in this study is 138%, which corresponds to the sample with 2.4 nm MgO (inset of Fig. 1).

To study the magnetic properties of the junctions, multilayers consisting of W(6)/Ru(10)/W(9)/$Co_{20}Fe_{60}B_{20}$(t)/MgO(2)/Ta(6) with $Co_{20}Fe_{60}B_{20}$ thicknesses (t) ranging from 0.8 to 2 nm were fabricated and annealed at 300 °C and 420 °C for 10 min. Ru is widely used in the buffer layers of MTJs, to reduce the resistivity of MTJ bottom electrode and enhance the PMA and crystallinity of CoFeB.[38–43] We estimated the interfacial magnetic anisotropy by fitting a linear curve to the anisotropy energy (in the form of $K_{eff} \cdot t_{CFB}$), versus CoFeB thickness, and finding the Y intercept of the fitted line as shown in Fig. 2. Interfacial perpendicular energy densities of 1.23 and 1.67 erg/cm^2 were obtained for annealing at 300 °C and 420 °C, respectively. These values are larger than the value (1.19 erg/cm^2) obtained in Ref. 32, but smaller than average K_i of 1.7 erg/cm^2 reported in Ref. 29. From the areal saturation magnetization versus CoFeB thickness for the case of 420 °C [see Fig. S1 of the supplementary material], we found the thickness of dead layer and saturation magnetization to be 0.1 nm and 1350 emu/cc, respectively. It should be pointed out that we did not take into account this dead layer thickness for the calculation of K_i in Figs. 2(a) and 2(b). The K_i will increase from 1.67 to 1.85 erg/cm^2 if the dead layer is considered.

To compare W-based pMTJ with conventional Ta-based pMTJ, we investigated the evolution of conductance and TMR in both types of junctions during annealing. In addition, the comparison was made with Ta in-plane MTJs. Tunneling magnetoresistance of 600% has been demonstrated in Ta/CoFeB/MgO junctions with in-plane magnetic anisotropy.[35] However, the perpendicular counterpart with thin CoFeB layers exhibited much smaller TMR of ~160%.[7,37] The giant TMR in MTJs with in-plane magnetic anisotropy is developed in two different stages during the annealing process.[44] The first stage involves with the formation of highly conducting Δ_1 channel through the crystallization of amorphous CoFeB electrodes, corresponding to a sharp rise of TMR during initial annealing. The second stages involves with the improvement of crystalline structure of MgO (001) barrier, corresponding to a slower increase of TMR approaching to a saturation. Comparison of these behaviors could provide a unique opportunity to understand the limit of TMR in pMTJs.

The annealing study for W and Ta-based pMTJs was carried out at 340 °C, 380 °C, and 420 °C. The results for 340 °C and 380 °C showed a minor difference between these two types of samples (about 10% higher TMR is obtained for W-based pMTJs). Significantly different TMR behavior was observed for annealing at 420 °C. The evolution of TMR at this temperature is shown in Fig. 3(a) for W-pMTJ,

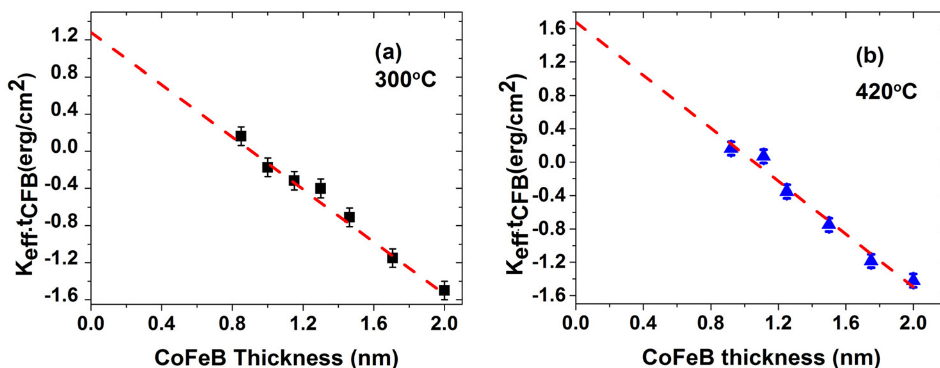

FIG. 2. Perpendicular anisotropy energy in the form of $K_{eff} \cdot t_{CFB}$ for different thickness of CoFeB (CFB). The red dashed lines are the linear fits to the data to estimate interfacial anisotropy energy (K_i). By finding the Y intercept, the values of 1.23 and 1.67 erg/cm^2 were obtained, respectively, for annealing at 300 °C and 420 °C for 10 min. Samples have the structure of W(6)/Ru(10)/W(9)/$Co_{20}Fe_{60}B_{20}$(t)/MgO(2)/Ta(6), where t had the values between 0.8 and 2.0 nm.

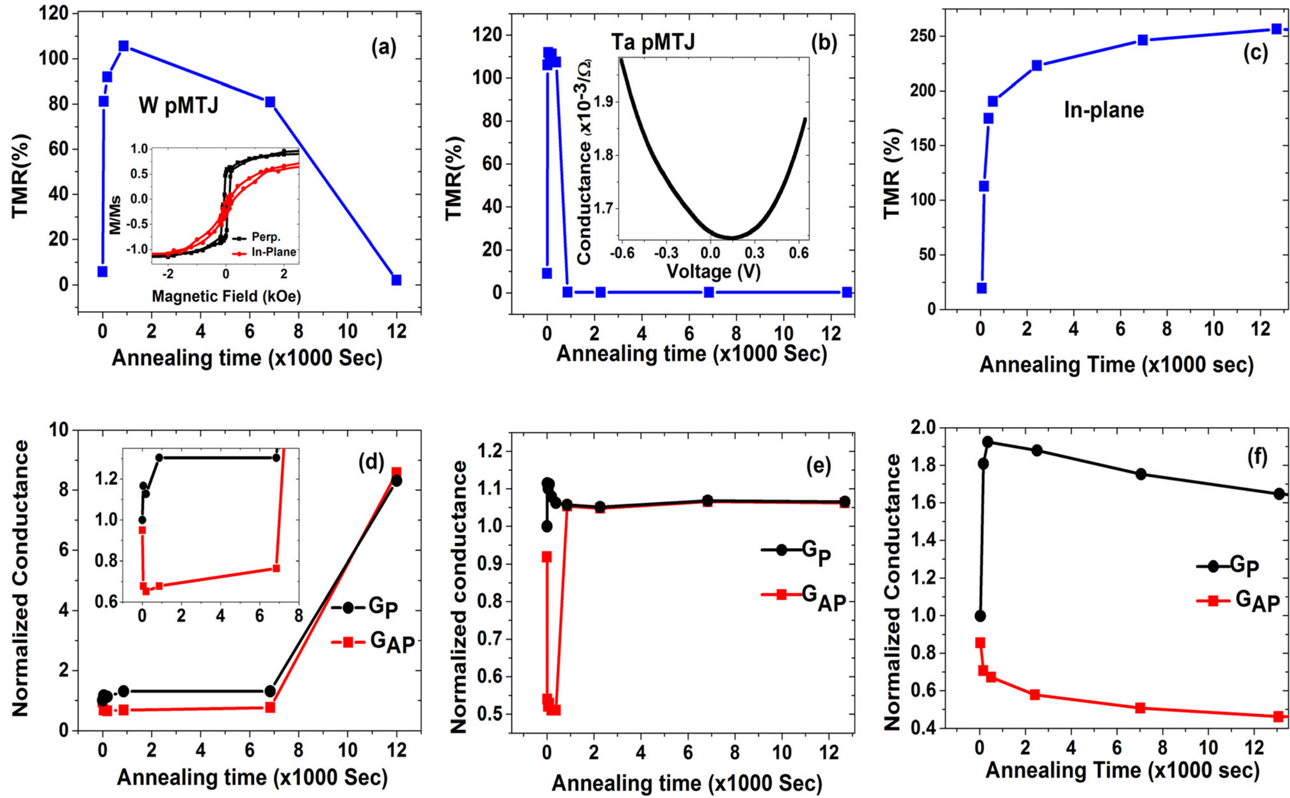

FIG. 3. Tunneling magnetoresistance curves (blue lines) versus annealing time for W-pMTJ (a), Ta-pMTJ (b), and Ta in-plane MTJ (c) structures, and corresponding normalized conductance for parallel state (G_P) (black lines) and antiparallel state (G_{AP}) (red lines) curves versus the time of annealing for W-pMTJ (d), Ta-pMTJ (e), and Ta in-plane MTJ (f) structures for annealing at 420 °C. Figure (f) is "Reprinted with permission from Wang *et al.*, Phys. Rev. B **81**, 144406 (2010). Copyright 2017 American Physical Society." The inset in (a) shows normalized magnetization (M/M_s) versus applied external field, in a direction parallel to the sample (red curves) and perpendicular to the sample (black curves) for W-pMTJ annealed at 420 °C for 6840 s. The inset in Fig. 3(b) shows bias dependence of parallel conductance channel of a perpendicular magnetic tunnel junction with MgO thickness of 1.2 nm. The inset of (d) shows the detailed evolution of conductance of W-pMTJ before MgO barrier fails.

Fig. 3(b) for Ta-pMTJ, and Fig. 3(c) for Ta in-plane junction, with the corresponding parallel conductance (G_p) and antiparallel conductance (G_{ap}) shown in the lower panels [Figs. 3(d)–3(f)]. Both pMTJs have the resistance area (RA) product of about 0.5 $M\Omega\,\mu m^2$ in parallel state. They have similar layers of CoFeB(0.85)/MgO(2)/CoFeB(1.6) in their structures. The data for the in-plane MTJ is from Ref. 44 (with written permission) and the structure of the sample is Si/SiO_2/Ta (7)/Ru (20)/Ta (7)/CoFe (2)/IrMn (15)/CoFe (2)/Ru (1.7)/CoFeB (3)/MgO (2)/CoFeB (3)/Ta (8)/Ru (10) with unit in nm.

First let us focus on the two pMTJs. The TMR experiences a sharp increase in both systems, reaching more than 80% after 12 s of annealing at 420 °C. For W-pMTJ, TMR reaches a peak value of 110% after annealing for 860 s then starts gradually decreasing upon further annealing as shown in Fig. 3(a). The TMR of Ta-pMTJ, on the other hand, reaches about ∼110% at the beginning then quickly drops nearly zero after 480 s. The evolution of G_p and G_{ap} in these two types of pMTJs provides more information on the very different behaviors. It can be seen that the drop of TMR in W-pMTJ to about 80% at 6840 s is mainly due to the slight increase of G_{ap} as shown in the inset of Fig. 3(d). Indeed, PMA at this annealing time is fully preserved as demonstrated in the hysteresis loops in the inset of Fig. 3(a). However, the fast decrease of TMR afterwards to nearly zero is due to the sudden increase of *both* G_p and G_{ap} as shown in Fig. 3(d), suggesting the collapsing of MgO tunnel barrier in extended annealing. Very interestingly, the evolution of G_p and G_{ap} is markedly different in Ta-pMTJ. The sharp drop of TMR after 480 s is caused by the increase of G_{ap} to a value equal to G_p, due to loss of antiparallel plateau in the TMR curve. When magnetization of the soft layer lies in the plane direction (orthogonal to that of the hard layer), TMR drops to ∼50% of its maximum value, as shown previously.[36] The PMA is totally lost after annealing for 6840 s in Ta-pMTJ, where the hysteresis loops under both in-plane and perpendicular fields exhibit superparamagnetic-like shape. This is in sharp contrast with the W-pMTJ where a reasonably strong PMA (∼1.1×10^6 erg/cc) is still retained, demonstrating W is indeed a better choice for maintaining stronger PMA during high temperature annealing as shown in previous studies.[28–31] However, unlike in W-pMTJ where MgO barrier became nearly transparent, both G_p and G_{ap} of Ta-pMTJ stayed nearly constant even to the end of annealing at 3.5 h, which indicates the MgO barrier is more stable in Ta-pMTJ despite of loss of PMA during prolonged annealing. The 10 times increase of conductance in W-pMTJ suggests the MgO barrier has been compromised, presumably due to the interdiffusion of W into the tunnel barrier during extended annealing. It is worthy to mention that annealing experiments have been conducted at different MgO and

CoFeB thicknesses and similar results were obtained for Ta and W pMTJs.

Now let us pay attention to the difference between pMTJs and the in-plane MTJ. A number of interesting features can be observed. First, TMR in all three systems increases rapidly at the beginning stage of annealing, agreeing with the rapid crystallization of CoFeB at 420 °C.[44] Second, unlike that of W-pMTJ and Ta-pMTJ, the TMR in the in-plane junction did not drop after annealing of a few hundred seconds. Instead it maintained a slow positive rate of increase and eventually reached a maximal value of 255%, which is due to the defect reduction in MgO so that the conduction of Δ_5 and $\Delta_{2'}$ band electrons is further reduced in this second stage of annealing.[44] Third, and most importantly, the evolution of G_p is strikingly different in pMTJ and in-plane MTJ. Before it started to decrease, G_p increased by 30% and 15% in W-pMTJ and Ta-pMTJ, respectively, as shown in Figs. 3(d) and 3(e). This jump is much smaller compared to the 90% increase of G_p in the in-plane MTJ as shown in Fig. 3(f). The rapid increase of G_p in the in-plane junctions is attributed the establishment of coherent tunneling of Δ_1 band electrons.[44] The inset in Fig. 3(b) shows bias dependence of parallel conductance channel of a perpendicular magnetic tunnel junction with MgO thickness of 1.2 nm. The asymmetry of the curve is due to the different oxidation of CoFeB layers above and below the MgO barrier. Unlike the case of in plane MTJs where we expect the contribution of Δ_5 channels with the thin MgO barrier,[45] there is no local minima at around small voltages (<0.3 V) in G(V) curve. Therefore, we believe the coherent tunneling of Δ_1 is not well stabilized in pMTJs, just as the absence of the characteristic feature of Δ_5 as shown in Fig. 3(b). These results suggest that the low TMR in pMTJs is related to the incomplete formation of the highly conducting Δ_1 channel. In addition to the crystallization of CoFeB and improvement of MgO crystalline structure, one has to consider other factors such as the presence of resonant states and change of oxidation level at the FM/oxide interface in order to understand the behavior of tunneling conductance. Therefore, the exact origin of the smaller increase of G_p in pMTJ is not clear at present, and it is beyond the scope of this work. Nevertheless, this comparison provided us a unique insight to understand why the TMR is much lower in pMTJs.

To understand the collapse of tunneling resistance in W-pMTJ after prolonged annealing, we have carried out a High-Resolution Scanning Transmission Electron Microscopy (HRSTEM) study on the pMTJs annealed for 3.5 h at 420 °C. Cross-sectional annular bright field (ABF)-STEM image of full MTJ stack is presented for W [Fig. 4(a)] and Ta [Fig. 4(d)] samples. As it is clear from Fig. 4(a), W-pMTJ does not show clear interfaces between layers and individual layers cannot be completely identified due to high level of roughness of the sample. In contrast, Ta-pMTJ shows much more smooth interfaces that are clearly distinguishable as presented in Fig. 4(d). To extract more information about the properties of MgO barriers, high resolution ABF-STEM images are presented for W [Fig. 4(b)] and Ta [Fig. 4(e)] samples. The MgO barrier of W-pMTJ junction [Fig. 4(b)] has wavy interfaces that cannot be clearly distinguished from CoFeB. Furthermore, no crystalline structure was observed in the MgO layer. Unlike the W sample, Ta-pMTJ shows much more clear MgO interfaces with CoFeB layers. In addition, sizable lattice fringes are visible for Ta sample indicating good crystallinity of the MgO barrier. Besides the high roughness of the W junction witnessed here, interdiffusion of W into CoFeB/MgO/CoFeB layers is also observed from the Energy Dispersive Spectroscopy (EDS) mapping as illustrated in Fig. 4(c), where red pixels are scattered everywhere including CoFeB and MgO layers. This interdiffusion of W into the MgO barrier explains why the resistance of the junctions dropped nearly ten times after the prolonged annealing at 420 °C. The diffusion of W into the MgO barrier could also be revealed by studying the temperature dependence of TMR as proposed by Shang *et al.*[46] and Jansen *et al.*,[47] which will be reported in our forthcoming publications. On the contrary, from EDS analysis for the Ta sample shown in Fig. 4(f), no detectable Ta signal above the noise level is observed within the MgO layer, supporting the idea that Ta-pMTJ is structurally more robust than W-pMTJ after annealing at a high temperature for extended time. More information can be obtained by comparing these HRSTEM results to those of as deposited and optimally annealed pMTJs, which is a study underway.

To address different factors when comparing pMTJs with Ta and W buffer/capping layers, one can discuss as the following. First of all, as we pointed out in an earlier report,[7] the tendency of forming binary HM-FM alloys can be estimated by their heat of formations[48] which is tabulated for many heavy metals, and it has the values of −19 kJ/mol and

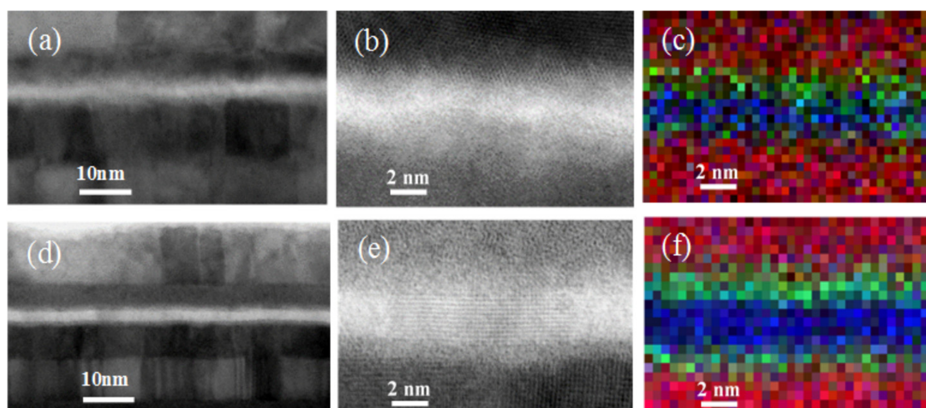

FIG. 4. Cross-sectional STEM image of the full pMTJ with W (a) and Ta (d), corresponding high resolution STEM images of MgO region for W (b) and Ta (e) junctions, and EDS mapping of pMTJs with W (c) and Ta (f), where Fe is in green, Mg is in blue and W (Ta) is in red.

−2.5 kJ/mol for Ta and W, respectively. Not surprisingly, Ta is more likely to form an alloy with Fe than W, which agrees also with the larger dead layer thickness observed in Ta samples reported by other papers.[29,32] The ability to absorb proper amount of boron, for the sake of CoFeB crystallization, is also a key factor that contributes to the formation of CoFeB(001)/MgO(001) interfaces.[49] Finally, the roughness and crystalline structure of HM layers is also very critical as revealed in the present study.

CONCLUSIONS

In summary, a large TMR of 138% was achieved in fully perpendicular MTJ with a simple W/CoFeB/MgO structure. Although W is a good material to promote strong PMA and large TMR when optimally annealed, it is less thermally stable compared to Ta if the annealing condition is not carefully chosen. Through a comparison study with conventional in-plane MTJ, the evolution of tunneling conductance suggests the relatively low TMR in pMTJs is related to the lack of highly polarized Δ_1 conducting channel developed in the initial stage of annealing.

SUPPLEMENTARY MATERIAL

See supplementary material for calculation of dead layer thickness and graphs of resistance area products of the samples with annealing time.

ACKNOWLEDGMENTS

This work was supported in part by C-SPIN, one of six centers of STARnet, a Semiconductor Research Corporation program, sponsored by MARCO and DARPA; and by the National Science Foundation through ECCS-1310338. The work was also supported in part by Inston, Inc., through a Phase II Small Business Innovation Research award from the National Science Foundation.

[1]N. Nishimura, T. Hirai, A. Koganei, T. Ikeda, K. Okano, Y. Sekiguchi, and Y. Osada, J. Appl. Phys. **91**, 5246 (2002).
[2]M. Yoshikawa, E. Kitagawa, T. Nagase, T. Daibou, M. Nagamine, K. Nishiyama, T. Kishi, and H. Yoda, IEEE Trans. Magn. **44**, 2573 (2008).
[3]K. Yakushiji, T. Saruya, H. Kubota, A. Fukushima, T. Nagahama, S. Yuasa, and K. Ando, Appl. Phys. Lett. **97**, 232508 (2010).
[4]K. Mizunuma, S. Ikeda, H. Sato, M. Yamanouchi, H. D. Gan, K. Miura, H. Yamamoto, J. Hayakawa, F. Matsukura, and H. Ohno, J. Appl. Phys. **109**, 07C711 (2011).
[5]A. Manchon, C. Ducruet, L. Lombard, S. Auffret, B. Rodmacq, B. Dieny, S. Pizzini, J. Vogel, V. Uhlíř, M. Hochstrasser, and G. Panaccione, J. Appl. Phys. **104**, 43914 (2008).
[6]S. Ikeda, K. Miura, H. Yamamoto, K. Mizunuma, H. D. Gan, M. Endo, S. Kanai, J. Hayakawa, F. Matsukura, and H. Ohno, Nat. Mater. **9**, 721 (2010).
[7]H. Almasi, D. R. Hickey, M. Xu, M. R. Rosales, S. Nahar, J. T. Held, K. A. Mkhoyan, and W. G. Wang, Appl. Phys. Lett. **106**, 182406 (2015).
[8]C. Grezes, F. Ebrahimi, J. G. Alzate, X. Cai, J. A. Katine, J. Langer, B. Ocker, P. Khalili, and K. L. Wang, Appl. Phys. Lett. **108**, 012403 (2016).
[9]S. Kanai, F. Matsukura, and H. Ohno, Appl. Phys. Lett. **108**, 192406 (2016).
[10]Y. Shiota, T. Nozaki, F. Bonell, S. Murakami, T. Shinjo, and Y. Suzuki, Nat. Mater. **11**, 39 (2012).
[11]T. Maruyama, Y. Shiota, T. Nozaki, K. Ohta, N. Toda, M. Mizuguchi, A. A. Tulapurkar, T. Shinjo, M. Shiraishi, S. Mizukami, Y. Ando, and Y. Suzuki, Nat. Nanotechnol. **4**, 158 (2009).
[12]M. Endo, S. Kanai, S. Ikeda, F. Matsukura, and H. Ohno, Appl. Phys. Lett. **96**, 212503 (2010).
[13]W.-G. Wang, M. Li, S. Hageman, and C. L. Chien, Nat. Mater. **11**, 64 (2012).
[14]M. K. Niranjan, C.-G. Duan, S. S. Jaswal, and E. Y. Tsymbal, Appl. Phys. Lett. **96**, 222504 (2010).
[15]C. Bi, Y. Liu, T. Newhouse-Illige, M. Xu, M. Rosales, J. W. Freeland, O. Mryasov, S. Zhang, S. G. E. te Velthuis, and W. G. Wang, Phys. Rev. Lett. **113**, 267202 (2014).
[16]U. Bauer, L. Yao, A. Tan, P. Agrawal, S. Emori, H. L. Tuller, S. van Dijken, and G. S. D. Beach, Nat. Mater. **14**, 174 (2015).
[17]W. H. Butler, X.-G. Zhang, T. C. Schulthess, and J. M. MacLaren, Phys. Rev. B **63**, 54416 (2001).
[18]D. D. Djayaprawira, K. Tsunekawa, M. Nagai, H. Maehara, S. Yamagata, N. Watanabe, S. Yuasa, Y. Suzuki, and K. Ando, Appl. Phys. Lett. **86**, 92502 (2005).
[19]L. Thomas, G. Jan, J. Zhu, H. Liu, Y.-J. Lee, S. Le, R.-Y. Tong, K. Pi, Y.-J. Wang, D. Shen, R. He, J. Haq, J. Teng, V. Lam, K. Huang, T. Zhong, T. Torng, and P.-K. Wang, J. Appl. Phys. **115**, 172615 (2014).
[20]M. Gottwald, J. J. Kan, K. Lee, X. Zhu, C. Park, and S. H. Kang, Appl. Phys. Lett. **106**, 32413 (2015).
[21]Y. W. Oh, K. D. Lee, J. R. Jeong, and B. G. Park, J. Appl. Phys. **115**, 17C724 (2014).
[22]T. Liu, J. W. Cai, and L. Sun, AIP Adv. **2**, 32151 (2012).
[23]M. Akyol, G. Yu, J. G. Alzate, P. Upadhyaya, X. Li, K. L. Wong, A. Ekicibil, P. Khalili Amiri, and K. L. Wang, Appl. Phys. Lett. **106**, 162409 (2015).
[24]C. F. Pai, M. H. Nguyen, C. Belvin, L. H. Vilela-Leão, D. C. Ralph, and R. A. Buhrman, Appl. Phys. Lett. **104**, 82407 (2014).
[25]T. Liu, Y. Zhang, J. W. Cai, and H. Y. Pan, Sci. Rep. **4**, 5895 (2014).
[26]X. Li, G. Yu, H. Wu, P. V. Ong, K. Wong, Q. Hu, F. Ebrahimi, P. Upadhyaya, M. Akyol, N. Kioussis, X. Han, P. Khalili Amiri, and K. L. Wang, Appl. Phys. Lett. **107**, 142403 (2015).
[27]K. Watanabe, S. Fukami, H. Sato, F. Matsukura, and H. Ohno, IEEE Trans. Magn. **52**, 3400904 (2016).
[28]J.-H. Kim, J.-B. Lee, G.-G. An, S.-M. Yang, W.-S. Chung, H.-S. Park, and J.-P. Hong, Sci. Rep. **5**, 16903 (2015).
[29]G.-G. An, J.-B. Lee, S.-M. Yang, J.-H. Kim, W.-S. Chung, and J.-P. Hong, Acta Mater. **87**, 259 (2015).
[30]A. Kaidatzis, C. Bran, V. Psycharis, M. Vázquez, J. M. García-Martín, and D. Niarchos, Appl. Phys. Lett. **106**, 262401 (2015).
[31]Q. Hao and G. Xiao, Phys. Rev. Appl. **3**, 34009 (2015).
[32]W. Skowroński, T. Nozaki, D. D. Lam, Y. Shiota, K. Yakushiji, H. Kubota, A. Fukushima, S. Yuasa, and Y. Suzuki, Phys. Rev. B **91**, 184410 (2015).
[33]N. Tezuka, S. Oikawa, I. Abe, M. Matsuura, S. Sugimoto, K. Nishimura, and T. Seino, IEEE Magn. Lett. **7**, 3104204 (2016).
[34]S. Lee, Y. Takemura, J. Park, S. Lee, Y. Takemura, and J. Park, Appl. Phys. Lett. **109**, 182405 (2016).
[35]S. Ikeda, J. Hayakawa, Y. Ashizawa, Y. M. Lee, K. Miura, H. Hasegawa, M. Tsunoda, F. Matsukura, and H. Ohno, Appl. Phys. Lett. **93**, 82508 (2008).
[36]W.-G. Wang, S. Hageman, M. Li, S. Huang, X. Kou, X. Fan, J. Q. Xiao, and C. L. Chien, Appl. Phys. Lett. **99**, 102502 (2011).
[37]H. D. Gan, H. Sato, M. Yamanouchi, S. Ikeda, K. Miura, R. Koizumi, F. Matsukura, and H. Ohno, Appl. Phys. Lett. **99**, 252507 (2011).
[38]M. Yamanouchi, R. Koizumi, S. Ikeda, H. Sato, K. Mizunuma, K. Miura, H. D. Gan, F. Matsukura, and H. Ohno, J. Appl. Phys. **109**, 07C712 (2011).
[39]M. Frankowski, A. Żywczak, M. Czapkiewicz, S. Zietek, J. Kanak, M. Banasik, W. Powroźnik, W. Skowroński, J. Chęciński, J. Wrona, H. Głowiński, J. Dubowik, J.-P. Ansermet, and T. Stobiecki, J. Appl. Phys. **117**, 223908 (2015).
[40]S. Y. Jang, S. H. Lim, and S. R. Lee, J. Appl. Phys. **107**, 09C707 (2010).
[41]Y. M. Lee, J. Hayakawa, S. Ikeda, F. Matsukura, and H. Ohno, Appl. Phys. Lett. **89**, 42506 (2006).
[42]C. Park, Y. Wang, and J. Zhu, in *INTERMAG 2006-IEEE International Magnetics Conference* (2006), Vol. 42, p. 860.
[43]D. Wang, C. Nordman, J. M. Daughton, Z. Qian, and J. Fink, IEEE Trans. Magn. **40**, 2269 (2004).
[44]W. G. Wang, C. Ni, G. X. Miao, C. Weiland, L. R. Shah, X. Fan, P. Parson, J. Jordan-sweet, X. M. Kou, Y. P. Zhang, R. Stearrett, E. R. Nowak, R. Opila, J. S. Moodera, and J. Q. Xiao, Phys. Rev. B **81**, 144406 (2010).

[45]C. Tiusan, F. Greullet, M. Hehn, F. Montaigne, S. Andrieu, and A. Schuhl, J. Phys. Condens. Matter **19**, 165201 (2007).
[46]C. Shang, J. Nowak, R. Jansen, and J. Moodera, Phys. Rev. B **58**, R2917 (1998).
[47]R. Jansen and J. Moodera, Phys. Rev. B **61**, 9047 (2000).
[48]F. R. d. Boer, *Cohesion in Metals* (North-Holland, Amesterdam, 1988), pp. 412–548.
[49]T. Miyajima, T. Ibusuki, S. Umehara, M. Sato, S. Eguchi, M. Tsukada, and Y. Kataoka, Appl. Phys. Lett. **94**, 122501 (2009).